Computers and Mathematics with Applications 64 (2012) 2765–2774

Contents lists available at SciVerse ScienceDirect

Computers and Mathematics with Applications

journal homepage: www.elsevier.com/locate/camwa

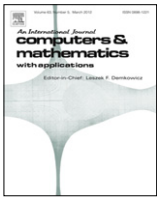

# Computational bases for $RT_k$ and $BDM_k$ on triangles

V.J. Ervin

*Department of Mathematical Sciences, Clemson University, Clemson, SC, 29634-0975, USA*

ARTICLE INFO

*Article history:*
Received 14 August 2012
Accepted 23 August 2012
Communicated by *Norbert Heuer*

*Keywords:*
$RT_k$ basis
$BDM_k$ basis
Piola transformation

ABSTRACT

In this article, we derive computational bases for Raviart–Thomas ($RT$) and Brezzi–Douglas–Marini ($BDM$) (vector) approximation spaces on a triangulation of a domain in $\mathbb{R}^2$. The basis functions, defined on the reference triangle, have a Lagrangian property. The continuity of the normal component of the approximation across the edges in the triangulation is satisfied by the use of the Piola transformation and the Lagrangian property of the basis functions. A numerical example is given demonstrating the approximation property of the bases.



## 1. Introduction

In this article we present computational bases for the Raviart–Thomas ($RT$) and Brezzi–Douglas–Marini ($BDM$) vector spaces on a triangulation of a domain $\Omega \subset \mathbb{R}^2$. The $RT$ and $BDM$ spaces are commonly used as approximation spaces for $H_{\text{div}}(\Omega) := \{\mathbf{u} \in \left(L^2(\Omega)\right)^2 \mid \nabla \cdot \mathbf{u} \in L^2(\Omega)\}$. The $H_{\text{div}}(\Omega)$ space frequently arises in mixed and dual-mixed variational formulations of the solution to partial differential equations. Let $\mathcal{T}_h$ denote a regular triangulation of $\Omega$, $\mathcal{E}_h = \{e_{ij} \mid e_{ij} = \partial T_i \cap \partial T_j, T_i, T_j \in \mathcal{T}_h, i \neq j\}$ (i.e. the interior edges of the triangulation $\mathcal{T}_h$), and $P_k(T)$ denote the space of bivariate polynomials of degree $\leq k$ on $T$. Then

$$RT_k(T) := (P_k(T))^2 + \mathbf{x}\, P_k(T), \tag{1.1}$$

and the $RT_k$ approximation space is defined by

$$RT_k(\Omega) := \{\mathbf{u}_h \mid \mathbf{u}_h \in RT_k(T)\ \forall T \in \mathcal{T}_h, \mathbf{u}_h \cdot \mathbf{n}_{ij} \text{ is continuous across } e_{ij}, \forall e_{ij} \in \mathcal{E}_h\}, \tag{1.2}$$

where $\mathbf{n}_{ij}$ is a unit normal vector to $e_{ij}$. The $BDM_k(\Omega)$ approximating space is defined by: $BDM_k(T) := (P_k(T))^2$,

$$BDM_k(\Omega) := \{\mathbf{u}_h \mid \mathbf{u}_h \in BDM_k(T)\ \forall T \in \mathcal{T}_h, \mathbf{u}_h \cdot \mathbf{n}_{ij} \text{ is continuous across } e_{ij}, \forall e_{ij} \in \mathcal{E}_h\}. \tag{1.3}$$

In the usual description of the $RT_k$ and $BDM_k$ spaces the continuity of $\mathbf{u}_h \cdot \mathbf{n}_{ij}$ across $e_{ij} \in \mathcal{E}_h$ is depicted graphically by indicating degrees of freedom for $\mathbf{u}_h \cdot \mathbf{n}$ on the edges of $T \in \mathcal{T}_h$ (see [1]).

In typical Finite Element (FE) computations restrictions on the Test Space, such as continuity of the approximation, continuity of the approximation and its derivative, are implicitly imposed by the appropriate choice of the basis functions for the Test Space. Additionally, these basis functions have a Lagrangian property where they have the value one at their nodal point and vanish at the other nodal basis points. Computations are performed using an affine transformation which maps integrals over $T \in \mathcal{T}_h$ to integrals over the reference triangle $\widehat{T}$ on which the basis functions are defined.

Finite Element software packages which include $RT$ elements as an approximation choice typically only provide an $RT_0$ approximation choice. A detailed discussion of the computational implementation of $RT_0$ elements may be found in [2]. (In the latest release of FreeFEM [3], version 3.13, $RT_1$ and $BDM_1$ elements have been added.) Our interest in $RT_k$,

*E-mail address:* vjervin@clemson.edu.

0898-1221/$ – see front matter © 2012 Elsevier Ltd. All rights reserved.
doi:10.1016/j.camwa.2012.08.011

$k \geq 1$, approximations arose from the approximation of coupled Stokes–Darcy flow problems. A common choice for the velocity–pressure approximation in Stokes flow problems is the Taylor–Hood $P_2 - P_1$ pair, i.e. a quadratic approximation for the velocity components and a linear approximation for the pressure. The desire to have a quadratic approximation for the velocity throughout the coupled domain motivated our investigation into approximations using $RT_2$.

Regarding the computation using *RT* and *BDM* elements, using an affine transformation to map $T$ to $\widehat{T}$ is not appropriate. An affine transformation does not preserve orthogonality of vectors and is therefore not suitable for enforcing the continuity of $\mathbf{u}_h \cdot \mathbf{n}_{ij}$ across $e_{ij}$. Rather, as is well known, the Piola transformation mapping $T$ to $\widehat{T}$ should be used in order to implement the continuity of $\mathbf{u}_h \cdot \mathbf{n}_{ij}$ across $e_{ij}$.

In this article we derive computational bases for *RT* and *BDM* approximations. The basis functions are defined relative to the reference triangle $\widehat{T}$ and have a Lagrangian property. This approach differs from the work of Arnold et al. [4], in which they present an abstract framework for the geometric decomposition of *RT* and *BDM* spaces to form local bases for them on any triangle $T$ in the triangulation. Also of note are the hierarchic finite element bases for $H_{\text{div}}(\Omega)$ and $H_{curl}(\Omega)$ constructed by Ainsworth and Coyle [5] (see also [6]). In both [5,6], unlike the approach described herein, the bases for $H_{\text{div}}(\Omega)$ and $H_{curl}(\Omega)$ are constructed using a hierarchic basis for the $H^1(\Omega)$ space of scalar functions. In the following section we introduce the notation used and review the Piola transformation. In Section 3 explicit bases are given for $RT_0$, $RT_1$, $RT_2$, and the general $RT_k$ case. Bases for $BDM_1$, $BDM_2$ and $BDM_k$ are derived in Section 4. Section 5 contains, as a numerical illustration, an approximation to a Darcy flow problem. Results where the velocity is approximated using $RT_0$, $RT_1$, $RT_2$, $BDM_1$, and $BDM_2$ are given.

## 2. Notation

We denote by $P_k(\mathbb{R}^n)$ the space of polynomials in $n$ variables of degree $\leq k$, and for $T \subset \mathbb{R}^n$, $P_k(T)$ the restriction of $P_k(\mathbb{R}^n)$ to $T$. The reference triangle with vertices (0, 0), (1, 0), and (0, 1) is denoted $\widehat{T}$ (see Fig. 2.1).

From [1], the dimension of the space $RT_k(T)$ is $(k+1)(k+3)$, and the dimension of $BDM_k(T)$ is $(k+1)(k+2)$.

In describing the bases for $RT_k(T)$ and $BDM_k(T)$ we divide the basis functions into two classes: *Normal Basis Functions* and *Non-Normal Basis Functions*. The Non-Normal Basis Functions satisfy the property that their normal component is zero along each edge of $T$ (see (2.5)), whereas the normal component of the Normal Basis Functions does not vanish along each edge of $T$.

### 2.1. Normal Basis Functions

The Normal Basis Functions are partitioned into three subclasses, each subclass associated with an edge of $\widehat{T}$. The edge numbering of $\widehat{T}$ is: edge 1 refers to the edge opposite vertex (0, 0), edge 2 refers to the edge opposite vertex (1, 0), and edge 3 refers to the vertex opposite vertex (0, 1) (see Fig. 2.1). Normal Basis Functions associated with edge $[i]$ are denoted $\Phi_{\cdot}^{[i]}$.

### 2.2. Non-Normal Basis Functions

For $RT_k(\widehat{T})$ the Non-Normal Basis Functions are partitioned into two subclasses, denoted $\Phi_{\cdot}^{[4]}$ and $\Phi_{\cdot}^{[5]}$.

For $BDM_k(\widehat{T})$ the Non-Normal Basis Functions are better described as *Tangent Basis Functions* and *Interior Basis Functions*. The Tangent Basis Functions, analogous to the Normal Basis Functions, are partitioned into three subclasses, denoted $\Phi_{\cdot}^{[4]}$, $\Phi_{\cdot}^{[5]}$ and $\Phi_{\cdot}^{[6]}$, associated with edges 1, 2, and 3, respectively. There are two subclasses of Interior Basis Functions for $BDM_k(\widehat{T})$, denoted $\Phi_{\cdot}^{[7]}$ and $\Phi_{\cdot}^{[8]}$.

### 2.3. Property of the basis functions

Let $\mathbf{n}_k$, $k = 1, 2, 3$, denote the outer unit normals to the respective edges on $\widehat{T}$. We have that

$$\text{Normal Basis Functions: } \Phi_{\cdot}^{[i]} \cdot \mathbf{n}_k = 0, \quad \text{along edge } k,\ i, k = 1, 2, 3,\ i \neq k, \tag{2.4}$$

$$\text{Non-Normal Basis Functions: } \Phi_{\cdot}^{[i]} \cdot \mathbf{n}_k = 0, \quad \text{along edge } k,\ k = 1, 2, 3,\ i = 4, 5, \ldots, 8. \tag{2.5}$$

### 2.4. The Piola transformation

We use the Piola transformation to map functions defined in $RT_k(\widehat{T})$ (or $BDM_k(\widehat{T})$) to functions defined in $RT_k(T)$ (or $BDM_k(T)$).

Consider the affine function $F$ (see Fig. 2.1) mapping $\widehat{T}$ onto $T$.

We have

$$F : \begin{cases} x = x_1 + (x_2 - x_1)\xi + (x_3 - x_1)\eta \\ y = y_1 + (y_2 - y_1)\xi + (y_3 - y_1)\eta. \end{cases} \tag{2.6}$$

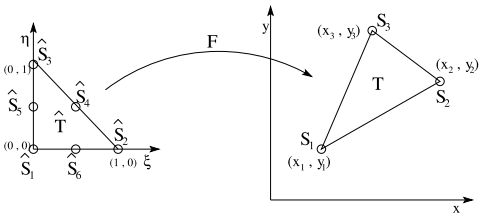


**Fig. 2.1.** Mapping of the reference triangle $\widehat{T}$ to the triangle $T$.

Let

$$J_T = \begin{bmatrix} \dfrac{\partial x}{\partial \xi} & \dfrac{\partial x}{\partial \eta} \\ \dfrac{\partial y}{\partial \xi} & \dfrac{\partial y}{\partial \eta} \end{bmatrix} = \begin{bmatrix} (x_2 - x_1) & (x_3 - x_1) \\ (y_2 - y_1) & (y_3 - y_1) \end{bmatrix}, \quad \text{and} \quad |J_T| = |\det(J_T)|.$$

The Piola transformation $\mathcal{P} : L^2(\widehat{T}) \longrightarrow L^2(T)$ is defined by

$$\hat{\mathbf{q}} \longmapsto \mathbf{q}(x) = \mathcal{P}(\hat{\mathbf{q}})(x) := \frac{1}{|J_T|} J_T \hat{\mathbf{q}}(\hat{x}). \tag{2.7}$$

The Piola transformation has the following properties [1,7]:

**Lemma 1.** *For $\hat{\mathbf{q}} \in C^1(\widehat{T})$, we have that $\mathbf{q} = \mathcal{P}(\hat{\mathbf{q}}) \in C^1(T)$, and*

$$\nabla_{x,y} \mathbf{q} = \frac{1}{|J_T|} J_T \nabla_{\xi,\eta} \hat{\mathbf{q}} J_T^{-1}, \quad \textit{and} \quad \nabla_{x,y} \cdot \mathbf{q} = \frac{1}{|J_T|} \nabla_{\xi,\eta} \cdot \hat{\mathbf{q}}. \tag{2.8}$$

**Lemma 2.** *For $\hat{v} \in H^1(\widehat{T})$, $\hat{\mathbf{q}}, \hat{\mathbf{p}} \in H_{\text{div}}(\widehat{T})$, $v := \hat{v} \circ F^{-1}$, $\mathbf{p} = \mathcal{P}(\hat{\mathbf{p}})$, and $\mathbf{q} = \mathcal{P}(\hat{\mathbf{q}})$ then*

$$\int_T \mathbf{q} \cdot \nabla_{x,y} v \, d\mathbf{x} = \int_{\widehat{T}} \hat{\mathbf{q}} \cdot \nabla_{\xi,\eta} \hat{v} \, d\boldsymbol{\xi}, \tag{2.9}$$

$$\int_T \nabla_{x,y} \cdot \mathbf{q} \, v \, d\mathbf{x} = \int_{\widehat{T}} \nabla_{\xi,\eta} \cdot \hat{\mathbf{q}} \, \hat{v} \, d\boldsymbol{\xi}, \tag{2.10}$$

$$\int_{\partial T} \mathbf{q} \cdot \mathbf{n} \, v \, ds = \int_{\partial \widehat{T}} \hat{\mathbf{q}} \cdot \mathbf{n} \, \hat{v} \, d\hat{s}, \tag{2.11}$$

$$\int_T \mathbf{p} \cdot \mathbf{q} \, d\mathbf{x} = \int_{\widehat{T}} J_T \hat{\mathbf{p}} \cdot J_T \hat{\mathbf{q}} \, \frac{1}{|J_T|} \, d\boldsymbol{\xi}. \tag{2.12}$$

*Important Remark*. There are a number of affine mappings of a triangle $T$ with vertices $V_1, V_2, V_3$, to $\widehat{T}$. From Fig. 2.1 the association $S_1 = V_1, S_2 = V_2, S_3 = V_3$, defines one such mapping. Another is given by the association $S_1 = V_2, S_2 = V_3$, $S_3 = V_1$. In order that $\mathbf{u}_h \cdot \mathbf{n}$ is continuous across the edges of the interior edges of the triangulation we have the following restriction on the choice of the mapping of $T$ to $\widehat{T}$. Suppose that $e_{ij}$ is a shared edge between triangles $T_i$ and $T_j$, and that under the mapping of $T_i$ to $\widehat{T}$ $e_{ij}$ maps to edge 1 of $\widehat{T}$, i.e. the edge of $\widehat{T}$ of length $\sqrt{2}$. Then the mapping of $T_j$ to $\widehat{T}$ must also map $e_{ij}$ to edge 1. This does not restrict the triangulation, only the choice of the association of $S_1, S_2, S_3$ with the vertices of $T$.

## 3. Basis functions for $RT_k(T)$

Introduce the following functions:

$$\hat{\mathbf{e}}_1(\xi, \eta) = \sqrt{2} \begin{bmatrix} \xi \\ \eta \end{bmatrix}, \qquad \hat{\mathbf{e}}_2(\xi, \eta) = \begin{bmatrix} \xi - 1 \\ \eta \end{bmatrix}, \qquad \hat{\mathbf{e}}_3(\xi, \eta) = \begin{bmatrix} \xi \\ \eta - 1 \end{bmatrix}, \tag{3.1}$$

$$\hat{\mathbf{e}}_4(\xi, \eta) = \eta \begin{bmatrix} \xi \\ \eta - 1 \end{bmatrix}, \qquad \hat{\mathbf{e}}_5(\xi, \eta) = \xi \begin{bmatrix} \xi - 1 \\ \eta \end{bmatrix}. \tag{3.2}$$

### 3.1. Basis for $RT_0(\widehat{T})$

The dimension of $RT_0(\widehat{T})$ is 3. There are no Non-Normal Basis Functions. The Normal Basis Functions are:

$$\Phi_1^{[1]}(\xi,\eta)=\hat{\mathbf{e}}_1(\xi,\eta),\qquad \Phi_1^{[2]}(\xi,\eta)=\hat{\mathbf{e}}_2(\xi,\eta),\qquad \Phi_1^{[3]}(\xi,\eta)=\hat{\mathbf{e}}_3(\xi,\eta). \tag{3.3}$$

Observe that for $\hat{\mathbf{g}}_j$ denoting the midpoint along edge $[j]$,

$$\Phi_1^{[i]}(\hat{\mathbf{g}}_j)\cdot\mathbf{n}_i=\begin{cases}1, & \text{if } j=i,\\ 0, & \text{if } j\neq i.\end{cases} \tag{3.4}$$

Note that $\Phi_1^{[i]}$, $i=1,2,3$, are in $RT_0(\widehat{T})$, and by property (3.4) the functions are linearly independent. As $\dim(RT_0(\widehat{T}))$ is 3, then it follows that the $\Phi_1^{[i]}$, $i=1,2,3$ form a basis for $RT_0(\widehat{T})$.

### 3.2. Basis for $RT_1(\widehat{T})$

The dimension of $RT_1(\widehat{T})$ is 8. There are six Normal Basis Functions, two associated with each side, and two Non-Normal Basis Functions.

Let $g_1=1/2-\sqrt{3}/6, g_2=1/2+\sqrt{3}/6$ denote the two Gaussian quadrature points on the interval $[0,1]$. Introduce the two linear Lagrangian polynomials associated with the Gaussian quadrature points

$$l_1(t):=\frac{(t-g_2)}{(g_1-g_2)},\quad\text{and}\quad l_2(t):=\frac{(t-g_1)}{(g_2-g_1)}. \tag{3.5}$$

The Normal Basis Functions are (defined in a counter clockwise orientation):

$$\Phi_1^{[1]}(\xi,\eta)=l_1(\eta)\,\hat{\mathbf{e}}_1(\xi,\eta),\qquad \Phi_2^{[1]}(\xi,\eta)=l_2(\eta)\,\hat{\mathbf{e}}_1(\xi,\eta), \tag{3.6}$$

$$\Phi_1^{[2]}(\xi,\eta)=l_2(\eta)\,\hat{\mathbf{e}}_2(\xi,\eta),\qquad \Phi_2^{[2]}(\xi,\eta)=l_1(\eta)\,\hat{\mathbf{e}}_2(\xi,\eta), \tag{3.7}$$

$$\Phi_1^{[3]}(\xi,\eta)=l_1(\xi)\,\hat{\mathbf{e}}_3(\xi,\eta),\qquad \Phi_2^{[3]}(\xi,\eta)=l_2(\xi)\,\hat{\mathbf{e}}_3(\xi,\eta). \tag{3.8}$$

The Non-Normal Basis Functions are:

$$\Phi_1^{[4]}(\xi,\eta)=\hat{\mathbf{e}}_4(\xi,\eta),\qquad \Phi_1^{[5]}(\xi,\eta)=\hat{\mathbf{e}}_5(\xi,\eta). \tag{3.9}$$

Note that the Normal Basis Functions have a Lagrangian property that along the boundary $\Phi_j^{[i]}\cdot\mathbf{n}$ vanishes at all but one of the Gaussian quadrature points. Also, as both Non-Normal Basis Functions satisfy $\Phi_1^{[i]}\cdot\mathbf{n}=0$ along the boundary then it follows that the Normal Basis Functions are linearly independent. As the two Non-Normal Basis Functions are linearly independent then we have that the set of Normal and Non-Normal Basis Functions is linearly independent. Noting that the $\Phi_j^{[i]}$'s are all elements of $RT_1(\widehat{T})$ then the given Normal and Non-Normal Basis Functions must form a basis for $RT_1(\widehat{T})$.

**Remark.** The choice of $g_1, g_2$ as Gaussian quadrature points is simply for convenience of evaluating integrals along edges of the triangulation. For any choice of $g_1, g_2\in[0,1]$, $g_1\neq g_2$, the above construction generates a basis for $RT_1(\widehat{T})$.

### 3.3. Basis for $RT_2(\widehat{T})$

The dimension of $RT_1(\widehat{T})$ is 15. There are nine Normal Basis Function, three associated with each side, and six Non-Normal Basis Functions.

Let $g_1=1/2-\sqrt{15}/10, g_2=1/2, g_3=1/2+\sqrt{15}/10$ denote the three Gaussian quadrature points on the interval $[0,1]$. Introduce the three quadratic Lagrangian polynomials associated with the Gaussian quadrature points

$$q_1(t):=\frac{(t-g_2)(t-g_3)}{(g_1-g_2)(g_1-g_3)},\qquad q_2(t):=\frac{(t-g_1)(t-g_3)}{(g_2-g_1)(g_2-g_3)},\quad\text{and}\quad q_3(t):=\frac{(t-g_1)(t-g_2)}{(g_3-g_1)(g_3-g_2)}. \tag{3.10}$$

The Normal Basis Functions are (defined in a counter clockwise orientation):

$$\Phi_1^{[1]}(\xi,\eta)=q_1(\eta)\,\hat{\mathbf{e}}_1(\xi,\eta),\qquad \Phi_2^{[1]}(\xi,\eta)=q_2(\eta)\,\hat{\mathbf{e}}_1(\xi,\eta),\qquad \Phi_3^{[1]}(\xi,\eta)=q_3(\eta)\,\hat{\mathbf{e}}_1(\xi,\eta), \tag{3.11}$$

$$\Phi_1^{[2]}(\xi,\eta)=q_3(\eta)\,\hat{\mathbf{e}}_2(\xi,\eta),\qquad \Phi_2^{[2]}(\xi,\eta)=q_2(\eta)\,\hat{\mathbf{e}}_2(\xi,\eta),\qquad \Phi_3^{[2]}(\xi,\eta)=q_1(\eta)\,\hat{\mathbf{e}}_2(\xi,\eta), \tag{3.12}$$

$$\Phi_1^{[3]}(\xi,\eta)=q_1(\xi)\,\hat{\mathbf{e}}_3(\xi,\eta),\qquad \Phi_2^{[3]}(\xi,\eta)=q_2(\xi)\,\hat{\mathbf{e}}_3(\xi,\eta),\qquad \Phi_3^{[3]}(\xi,\eta)=q_3(\xi)\,\hat{\mathbf{e}}_3(\xi,\eta). \tag{3.13}$$

The Non-Normal Basis Functions are:

$$\Phi_1^{[4]}(\xi,\eta)=(1-\xi-\eta)\,\hat{\mathbf{e}}_4(\xi,\eta),\qquad \Phi_2^{[4]}(\xi,\eta)=\xi\,\hat{\mathbf{e}}_4(\xi,\eta),\qquad \Phi_3^{[4]}(\xi,\eta)=\eta\,\hat{\mathbf{e}}_4(\xi,\eta), \tag{3.14}$$

$$\Phi_1^{[5]}(\xi,\eta)=(1-\xi-\eta)\,\hat{\mathbf{e}}_5(\xi,\eta),\qquad \Phi_2^{[5]}(\xi,\eta)=\xi\,\hat{\mathbf{e}}_5(\xi,\eta),\qquad \Phi_3^{[5]}(\xi,\eta)=\eta\,\hat{\mathbf{e}}_5(\xi,\eta). \tag{3.15}$$

### 3.4. The general case: basis $RT_k(\widehat{T})$

The basis for the general case is constructed in a similar manner.

Let $g_n$, $n = 1, 2, \ldots, k+1$ denote the $k+1$ Gaussian quadrature points on the interval [0, 1], and $l_j(t)$ denote the Lagrangian polynomial of degree $k$ such that $l_j(g_n) = \begin{cases} 1, & \text{if } n = j, \\ 0, & \text{if } n \neq j. \end{cases}$

Also, let $\{b_i(\xi, \eta), i = 1, 2, \ldots, k(k+1)/2\}$ denote a basis for $P_{k-1}(\widehat{T})$.

The Normal Basis Functions.

Associated with edge 1 we have the basis functions:

$$\Phi_j^{[1]}(\xi, \eta) = l_j(\eta)\, \hat{\mathbf{e}}_1(\xi, \eta), \quad j = 1, 2, \ldots, k+1. \tag{3.16}$$

Associated with edge 2 we have the basis functions:

$$\Phi_j^{[2]}(\xi, \eta) = l_{k+2-j}(\eta)\, \hat{\mathbf{e}}_2(\xi, \eta), \quad j = 1, 2, \ldots, k+1. \tag{3.17}$$

Associated with edge 3 we have the basis functions:

$$\Phi_j^{[3]}(\xi, \eta) = l_j(\xi)\, \hat{\mathbf{e}}_3(\xi, \eta), \quad j = 1, 2, \ldots, k+1. \tag{3.18}$$

The Non-Normal Basis Functions are:

$$\Phi_j^{[4]}(\xi, \eta) = b_j(\xi, \eta)\, \hat{\mathbf{e}}_4(\xi, \eta), \quad j = 1, 2, \ldots, k(k+1)/2, \tag{3.19}$$

$$\Phi_j^{[5]}(\xi, \eta) = b_j(\xi, \eta)\, \hat{\mathbf{e}}_5(\xi, \eta), \quad j = 1, 2, \ldots, k(k+1)/2. \tag{3.20}$$

Note that the number of Normal Basis Functions plus the number of Non-Normal Basis Functions: $3(k+1)+2k(k+1)/2 = (k+1)(k+3) = \dim(RT_k(\widehat{T}))$.

The linear independence of the Normal Basis Functions follows from their Lagrangian property and the fact that the Non-Normal Basis Functions satisfy (2.5). Hence, to establish that (3.16)–(3.20) form a basis for $RT_k(\widehat{T})$ what remains is to show that the Non-Normal Basis Functions are linearly independent. A simple calculation shows that the only values for $(\xi, \eta)$ such that

$$C_1 \hat{\mathbf{e}}_4(\xi, \eta) + C_2 \hat{\mathbf{e}}_5(\xi, \eta) = \mathbf{0}$$

has a nontrivial solution for $C_1, C_2$ lie along the lines $\xi = 0$, $\eta = 0$, and $\xi + \eta = 1$.

Consider a linear combination of the Non-Normal Basis Functions, $\alpha_j, \beta_j \in \mathbb{R}$, $j = 1, 2, \ldots, N := k(k+1)/2$,

$$\begin{aligned} &(\alpha_1 b_1(\xi, \eta) + \alpha_2 b_2(\xi, \eta) + \cdots + \alpha_N b_N(\xi, \eta))\, \hat{\mathbf{e}}_4(\xi, \eta) \\ &\quad + (\beta_1 b_1(\xi, \eta) + \beta_2 b_2(\xi, \eta) + \cdots + \beta_N b_N(\xi, \eta))\, \hat{\mathbf{e}}_5(\xi, \eta) = \mathbf{0}. \end{aligned} \tag{3.21}$$

Without loss of generality, suppose that $\{b_i(\xi, \eta), i = 1, 2, \ldots, N\}$ is a Lagrangian basis with nodes, $\boldsymbol{\sigma}_j, j = 1, 2, \ldots, N$ lying strictly inside $\widehat{T}$, with $b_i(\boldsymbol{\sigma}_j) = \begin{cases} 1, & i = j, \\ 0, & i \neq j. \end{cases}$

Then, with $(\xi, \eta) = \boldsymbol{\sigma}_j$ (3.21) implies

$$\alpha_j \hat{\mathbf{e}}_4(\boldsymbol{\sigma}_j) + \beta_j \hat{\mathbf{e}}_5(\boldsymbol{\sigma}_j) = \mathbf{0}.$$

As noted above, this then implies that $\alpha_j = \beta_j = 0$. Hence the Non-Normal Basis Functions are linearly independent.

### 3.5. Basis for $RT_k(T)$

Note that from (2.7), (3.1), (3.2), for $i = 1, 2, 3$,

$$\mathbf{e}_i(x, y) = \mathcal{P}(\hat{\mathbf{e}}_i(F^{-1}(x, y))) = \begin{bmatrix} c_1 \\ c_2 \end{bmatrix} + \begin{bmatrix} x \\ y \end{bmatrix} c_3, \quad \text{where } c_1, c_2, c_3 \in P_0(T) = \mathbb{R}, \tag{3.22}$$

and for $i = 4, 5$,

$$\mathbf{e}_i(x, y) = \mathcal{P}(\hat{\mathbf{e}}_i(F^{-1}(x, y))) = \begin{bmatrix} p_1^i(x, y) \\ p_2^i(x, y) \end{bmatrix} + \begin{bmatrix} x \\ y \end{bmatrix} p_3^i(x, y), \tag{3.23}$$

where $p_1^i(x, y), p_2^i(x, y), p_3^i(x, y) \in P_1(T)$.

Also, for $\hat{p}(\xi, \eta) \in P_l(\widehat{T})$, then

$$\begin{aligned} \phi_k^{[i]}(x, y) &= \mathcal{P}(\Phi_k^{[i]}(F^{-1}(x, y))) = \mathcal{P}(\hat{p}(F^{-1}(x, y))\, \hat{\mathbf{e}}_i(F^{-1}(x, y))) \\ &= p(x, y)\, \mathcal{P}(\hat{\mathbf{e}}_i(F^{-1}(x, y))), \quad \text{where } p(x, y) \in P_l(T). \end{aligned} \tag{3.24}$$

**Theorem 1.** *Under the Piola transformation (2.7), the basis given for $RT_k(\widehat{T})$ transforms to a basis for $RT_k(T)$.*

**Proof.** The stated result follows from the definition of $RT_k(T)$, (1.1), and the properties (3.22)–(3.24). □

## 4. Basis functions for $BDM_k(T)$

Introduce the following *edge functions*. We suppress the dependence of the functions on $\xi$ and $\eta$.

$$\hat{\mathbf{e}}_1(s_1,s_2)=\frac{\sqrt{2}}{(s_2-s_1)}\begin{bmatrix}s_2\,\xi\\(s_2-1)\,\eta\end{bmatrix},\qquad \hat{\mathbf{e}}_2(s_1,s_2)=\frac{1}{(s_2-s_1)}\begin{bmatrix}s_2\xi+\eta-s_2\\(s_2-1)\,\eta\end{bmatrix},$$
$$\hat{\mathbf{e}}_3(s_1,s_2)=\frac{1}{(s_2-s_1)}\begin{bmatrix}(s_2-1)\,\xi\\\xi+s_2\eta-s_2\end{bmatrix},\qquad \hat{\mathbf{e}}_4(s_1,s_2)=(1-\xi-\eta)\hat{\mathbf{e}}_1(s_1,s_2),$$
$$\hat{\mathbf{e}}_5(s_1,s_2)=\xi\hat{\mathbf{e}}_2(s_1,s_2),\qquad \hat{\mathbf{e}}_6(s_1,s_2)=\eta\hat{\mathbf{e}}_3(s_1,s_2). \tag{4.1}$$

Let $\hat{\mathbf{b}}_1(\xi,\eta)$, $\hat{\mathbf{b}}_2(\xi,\eta)$ denote the interior bubble functions

$$\hat{\mathbf{b}}_1(\xi,\eta)=(1-\xi-\eta)\xi\eta\begin{bmatrix}1\\0\end{bmatrix},\qquad \hat{\mathbf{b}}_2(\xi,\eta)=(1-\xi-\eta)\xi\eta\begin{bmatrix}0\\1\end{bmatrix}. \tag{4.2}$$

Note that

$$\begin{array}{lll}\text{along edge 1}&\text{along edge 2}&\text{along edge 3}\\(\text{i.e. }\xi+\eta=1)&(\text{i.e. }\xi=0)&(\text{i.e. }\eta=0)\\\text{for }\eta=s_1,\hat{\mathbf{e}}_1\cdot\mathbf{n}_1=1,&\text{for }\eta=s_1,\hat{\mathbf{e}}_2\cdot\mathbf{n}_2=1,&\text{for }\xi=s_1,\hat{\mathbf{e}}_3\cdot\mathbf{n}_3=1,\\\text{for }\eta=s_2,\hat{\mathbf{e}}_1\cdot\mathbf{n}_1=0,&\text{for }\eta=s_2,\hat{\mathbf{e}}_2\cdot\mathbf{n}_2=0,&\text{for }\xi=s_2,\hat{\mathbf{e}}_3\cdot\mathbf{n}_3=0.\end{array} \tag{4.3}$$

Also, $\hat{\mathbf{e}}_i\cdot\mathbf{n}_j=0$, for $i=1,2,\ldots,6$, $j=1,2,3$, $i\neq j$, and $\hat{\mathbf{b}}_i(\xi,\eta)\cdot\mathbf{n}_j=0$, for $i=1,2$, $j=1,2,3$.

### 4.1. $BDM_1(\widehat{T})$

The dimension of $BDM_1(\widehat{T})$ is 6. The basis consists of six Normal Basis Functions.
Let $g_1=1/2-\sqrt{3}/6$, $g_2=1/2+\sqrt{3}/6$ denote the two Gaussian quadrature points on the interval [0, 1].
The basis functions (defined in a counter clockwise orientation) are:

$$\Phi_1^{[1]}(\xi,\eta)=\hat{\mathbf{e}}_1(g_1,g_2),\qquad \Phi_2^{[1]}(\xi,\eta)=\hat{\mathbf{e}}_1(g_2,g_1), \tag{4.4}$$
$$\Phi_1^{[2]}(\xi,\eta)=\hat{\mathbf{e}}_2(g_2,g_1),\qquad \Phi_2^{[2]}(\xi,\eta)=\hat{\mathbf{e}}_2(g_1,g_2), \tag{4.5}$$
$$\Phi_1^{[3]}(\xi,\eta)=\hat{\mathbf{e}}_3(g_1,g_2),\qquad \Phi_1^{[3]}(\xi,\eta)=\hat{\mathbf{e}}_3(g_2,g_1). \tag{4.6}$$

### 4.2. $BDM_2(\widehat{T})$

The dimension of $BDM_2(\widehat{T})$ is 12. The basis consists of nine Normal Basis Functions and three Tangent Basis Functions.
Let $l(z_1,z_2;t):=\frac{(t-z_2)}{(z_1-z_2)}$, represent the linear function which is equal to 1 when $t=z_1$, and equal to 0 when $t=z_2$.
Let $g_1=1/2-\sqrt{15}/10$, $g_2=1/2$, $g_3=1/2+\sqrt{15}/10$ denote the three Gaussian quadrature points on the interval [0, 1].
The Normal Basis Functions are (defined in a counter clockwise orientation):

$$\begin{aligned}&\Phi_1^{[1]}(\xi,\eta)=l(g_1,g_3;\eta)\,\hat{\mathbf{e}}_1(g_1,g_2),\qquad \Phi_2^{[1]}(\xi,\eta)=l(g_2,g_1;\eta)\,\hat{\mathbf{e}}_1(g_2,g_3),\\&\Phi_3^{[1]}(\xi,\eta)=l(g_3,g_2;\eta)\,\hat{\mathbf{e}}_1(g_3,g_1),\end{aligned} \tag{4.7}$$
$$\begin{aligned}&\Phi_1^{[2]}(\xi,\eta)=l(g_3,g_2;\eta)\,\hat{\mathbf{e}}_2(g_3,g_1),\qquad \Phi_2^{[2]}(\xi,\eta)=l(g_2,g_1;\eta)\,\hat{\mathbf{e}}_2(g_2,g_3),\\&\Phi_3^{[2]}(\xi,\eta)=l(g_1,g_3;\eta)\,\hat{\mathbf{e}}_2(g_1,g_2),\end{aligned} \tag{4.8}$$
$$\begin{aligned}&\Phi_1^{[3]}(\xi,\eta)=l(g_1,g_3;\xi)\,\hat{\mathbf{e}}_3(g_1,g_2),\qquad \Phi_2^{[3]}(\xi,\eta)=l(g_2,g_1;\xi)\,\hat{\mathbf{e}}_3(g_2,g_3),\\&\Phi_3^{[3]}(\xi,\eta)=l(g_3,g_2;\xi)\,\hat{\mathbf{e}}_3(g_3,g_1).\end{aligned} \tag{4.9}$$

The Tangent Basis Functions are:

$$\Phi_1^{[4]}(\xi,\eta)=\hat{\mathbf{e}}_4(g_1,g_2),\qquad \Phi_1^{[5]}(\xi,\eta)=\hat{\mathbf{e}}_5(g_1,g_2),\qquad \Phi_1^{[6]}(\xi,\eta)=\hat{\mathbf{e}}_6(g_1,g_2). \tag{4.10}$$

To establish that the $\Phi_j^{[i]}(\xi,\eta)$, defined in (4.7)–(4.10), form a basis for $BDM_2(\widehat{T})$ it suffices to show that $\Phi_1^{[4]}$, $\Phi_1^{[5]}$, $\Phi_1^{[6]}$, are linearly independent. Consider

$$\alpha_0\Phi_1^{[4]}(\xi,\eta)+\beta_0\Phi_1^{[5]}(\xi,\eta)+\gamma_0\Phi_1^{[6]}(\xi,\eta)=\mathbf{0}. \tag{4.11}$$

Along edge 1, the unit tangent is $\hat{\mathbf{t}} = \frac{1}{\sqrt{2}}\begin{bmatrix}-1\\1\end{bmatrix}$, and $\xi = 1-\eta$. Taking the dot product of (4.11) with respect to $\hat{\mathbf{t}}$, substituting $\xi = 1-\eta$, and simplifying we obtain the equation

$$\beta_0 - \gamma_0 = 0. \tag{4.12}$$

Along edge 2, the unit tangent is $\hat{\mathbf{t}} = \begin{bmatrix}0\\-1\end{bmatrix}$, and $\xi = 0$. Taking the dot product of (4.11) with respect to $\hat{\mathbf{t}}$, substituting $\xi = 0$, and simplifying we obtain the equation

$$\sqrt{2}(g_2 - 1)\alpha_0 - g_2\gamma_0 = 0. \tag{4.13}$$

Similarly, along edge 3, the unit tangent is $\hat{\mathbf{t}} = \begin{bmatrix}1\\0\end{bmatrix}$, and $\eta = 0$. Taking the dot product of (4.11) with respect to $\hat{\mathbf{t}}$, substituting $\eta = 0$, and simplifying we obtain the equation

$$\sqrt{2}\alpha_0 - \beta_0 = 0. \tag{4.14}$$

From (4.12) to (4.14) it follows that $\alpha_0 = \beta_0 = \gamma_0 = 0$.

Hence the $\Phi_j^{[i]}(\xi, \eta)$ form a basis for $BDM_2(\widehat{T})$.

### 4.3. The general case: $BDM_k(\widehat{T})$

The basis for the general case is constructed in a similar manner.

Let $g_n, n = 1, 2, \ldots, k+1$ denote the $k+1$ Gaussian quadrature points on the interval $[0, 1]$. Also, for ease of explanation of the basis, let $g_{k+1+i} = g_i$, $i = 1, 2, \ldots, k+1$.

Let $l_j(t)$ denote the Lagrangian polynomial of degree $k-1$, constructed using the $k$ points $g_j, g_{j+2}, g_{j+3}, \ldots, g_{j+k}$ such that $l_j(g_n) = \begin{cases}1, & \text{if } n = j,\\ 0, & \text{if } n = j+2, j+3, \ldots, j+k.\end{cases}$

Also, let $\{\rho_i(\xi), i = 0, 1, \ldots, (k-2)\}$ denote a basis for $P_{k-2}(\mathbb{R})$, and $\{v_i(\xi, \eta), i = 1, 2, \ldots, (k-2)(k-1)/2\}$ denote a basis for $P_{k-3}(\widehat{T})$.

The Normal Basis Functions.

Associated with Edge 1 we have the basis functions:

$$\Phi_j^{[1]}(\xi, \eta) = l_j(\eta)\,\hat{\mathbf{e}}_1(g_j, g_{j+1}), \quad j = 1, 2, \ldots, k+1. \tag{4.15}$$

Associated with Edge 2 we have the basis functions:

$$\Phi_j^{[2]}(\xi, \eta) = l_j(\eta)\,\hat{\mathbf{e}}_2(g_j, g_{j+1}), \quad j = k+1, k, \ldots, 1. \tag{4.16}$$

Associated with Edge 3 we have the basis functions:

$$\Phi_j^{[3]}(\xi, \eta) = l_j(\xi)\,\hat{\mathbf{e}}_3(g_j, g_{j+1}), \quad j = 1, 2, \ldots, k+1. \tag{4.17}$$

The Tangent Basis Functions are:

$$\Phi_j^{[4]}(\xi, \eta) = \rho_j(\eta)\,\hat{\mathbf{e}}_4(g_1, g_2), \qquad \Phi_j^{[5]}(\xi, \eta) = \rho_j(\xi)\,\hat{\mathbf{e}}_5(g_1, g_2), \qquad \Phi_j^{[6]}(\xi, \eta) = \rho_j(\eta)\,\hat{\mathbf{e}}_6(g_1, g_2), \tag{4.18}$$

$j = 0, 1, \ldots, k-2$.

The Interior Basis Functions are:

$$\Phi_j^{[7]}(\xi, \eta) = v_j(\xi, \eta)\,\hat{\mathbf{b}}_1(\xi, \eta), \qquad \Phi_j^{[8]}(\xi, \eta) = v_j(\xi, \eta)\,\hat{\mathbf{b}}_2(\xi, \eta), \quad j = 1, 2, \ldots, (k-2)(k-1)/2. \tag{4.19}$$

Note that the number of Normal Basis Functions plus Tangent Basis Functions plus Interior Basis Functions $= 3(k+1) + 3(k-1) + (k-2)(k-1) = (k+1)(k+2) = \dim(BDM_k)$.

The linear independence of the Normal Basis Functions follows from the Lagrangian property and the fact that the Non-Normal Basis Functions satisfy (2.5). To show that the Non-Normal Basis Functions are linearly independent first note that the Interior Basis Functions all vanish on the boundary of $\widehat{T}$. We proceed by considering a linear combination of the Tangent Basis Functions along the edges of $\widehat{T}$.

Let the linear combination of the Tangent Basis Functions be given by

$$\begin{aligned}&(\alpha_0 + \alpha_1\eta + \cdots + \alpha_{k-2}\eta^{k-2})\hat{\mathbf{e}}_4(g_1, g_2) + (\beta_0 + \beta_1\xi + \cdots + \beta_{k-2}\xi^{k-2})\hat{\mathbf{e}}_5(g_1, g_2)\\ &\quad + (\gamma_0 + \gamma_1\eta + \cdots + \gamma_{k-2}\eta^{k-2})\hat{\mathbf{e}}_6(g_1, g_2) = \mathbf{0}.\end{aligned} \tag{4.20}$$

As in the discussion above for the basis for $BDM_2$, we consider (4.20) along each of the edges of $\widehat{T}$.

Along edge 3 (i.e. $\hat{\mathbf{t}} = \begin{bmatrix}1\\0\end{bmatrix}$, $\eta = 0$) from (4.20) we have that

$$(\sqrt{2}\alpha_0 - \beta_0) - \beta_1\xi - \beta_2\xi^2 - \cdots - \beta_{k-2}\xi^{k-2} = 0,$$
$$\Longrightarrow \sqrt{2}\alpha_0 - \beta_0 = 0, \qquad \beta_j = 0, \quad j = 1, 2, \ldots, k-2. \tag{4.21}$$

With $\beta_j = 0, j = 1, 2, \ldots, k-2$, along edge 1 (i.e. $\hat{\mathbf{t}} = \frac{1}{\sqrt{2}}\begin{bmatrix}-1\\1\end{bmatrix}$, $\xi = 1 - \eta$), from (4.20) it follows that

$$\beta_0 - \gamma_0 = 0, \qquad \gamma_j = 0, \quad j = 1, 2, \ldots, k-2. \tag{4.22}$$

With $\gamma_j = 0, j = 1, 2, \ldots, k-2$, along edge 2 (i.e. $\hat{\mathbf{t}} = \begin{bmatrix}0\\-1\end{bmatrix}$, $\xi = 0$) from (4.20) it follows that

$$\sqrt{2}(g_2 - 1)\alpha_0 - g_2\gamma_0 = 0, \qquad \alpha_j = 0, \quad j = 1, 2, \ldots, k-2. \tag{4.23}$$

In view of (4.12)–(4.14) we also have $\alpha_0 = \beta_0 = \gamma_0 = 0$.
The linear independence of the Interior Basis Functions is obvious.
Hence the $\Phi_j^{[i]}(\xi, \eta)$ form a basis for $BDM_k(\widehat{T})$.

**Theorem 2.** *Under the Piola transformation (2.7), the basis given for $BDM_k(\widehat{T})$ transforms to a basis for $BDM_k(T)$.*

**Proof.** The stated result follows from the definition of $BDM_k(T)$, and that the Piola transformation is an affine invertible mapping. □

## 5. Numerical example

In this section we briefly discuss the numerical implementation and present a numerical example.

### 5.1. Numerical implementation

The numerical implementation of an approximation using the bases described above follows in a similar manner to the usual Finite Element computations with two caveats.

Recall that for a continuous (scalar) linear representation in Finite Elements we write

$$w_h(x, y) = \sum_k c_k \phi_k(x, y) = \sum_{T\in\mathcal{T}_h}\sum_{j=1}^{3} c_{\kappa(j,T)}\hat{l}_j(F^{-1}(x, y)), \tag{5.1}$$

where $\hat{l}_1 = 1 - \xi - \eta, \hat{l}_2 = \xi, \hat{l}_3 = \eta$, denote the basis functions on $\widehat{T}$, and $\kappa(j, T)$ denotes an index function. (See [8] for more details.)

Analogously we write

$$\mathbf{u}_h(x, y) = \sum_k c_k \boldsymbol{\phi}_k(x, y)$$
$$= \sum_{T\in\mathcal{T}_h}\left[\underbrace{\sum_{i=1}^{3}\sum_j c_{\kappa(i,j,T)} n\_\mathrm{sgn}(i, T)\mathcal{P}(\Phi_j^{[i]}(F^{-1}(x, y)))}_{\text{Normal Basis Functions}} + \underbrace{\sum_{i>3}\sum_j c_{\kappa(i,j,T)}\mathcal{P}(\Phi_j^{[i]}(F^{-1}(x, y)))}_{\text{Non-Normal Basis Functions}}\right], \tag{5.2}$$

where $\kappa(i, j, T)$ denotes an index function.

Let $e_{ij}$ denote the shared edge between triangles $T_i$ and $T_j$.

1. Sign associated with Normal Basis Functions

The respective Normal Basis Functions for $T_i$ and $T_j$ point in opposite directions across $e_{ij}$. In order that $\mathbf{u}_h \cdot \mathbf{n}$ is continuous across $e_{ij}$, we assign a (unit) normal direction to $e_{ij}$. If the outer (unit) normal to $T_i$ along $e_{ij}$ is the negative of the assigned normal then the corresponding Normal Basis Functions are multiplied by $-1$, otherwise they are multiplied by 1. We use the function $n\_\mathrm{sgn}(i, T) = \pm 1$ to represent this multiplicative factor associated with edge $i$ of triangle $T$.

2. Restriction of the mapping of $T$ to $\widehat{T}$

For $\mathbf{e}_i$ an edge of $T$ with outer normal $\mathbf{n}$, let $\hat{\mathbf{e}}_{iT} = F^{-1}(\mathbf{e}_i)$ denote the corresponding edge on $\widehat{T}$. Then, for $(x, y) \in \mathbf{e}_i$

$$\mathbf{u}_h \cdot \mathbf{n}\,(x, y) = \left[\sum_{i=1}^{3}\sum_j c_{\kappa(i,j,T)} n\_\mathrm{sgn}(i, T)\mathcal{P}(\Phi_j^{[i]}(F^{-1}(x, y)))\right] \cdot \mathbf{n}. \tag{5.3}$$

In particular for $(x, y) = \mathbf{g} = F(\hat{\mathbf{g}})$, $\hat{\mathbf{g}}$ a Gaussian point on $\hat{\mathbf{e}}_{iT}$, $\mathbf{n}_e = n\_\mathrm{sgn}(i, T)\mathbf{n}$

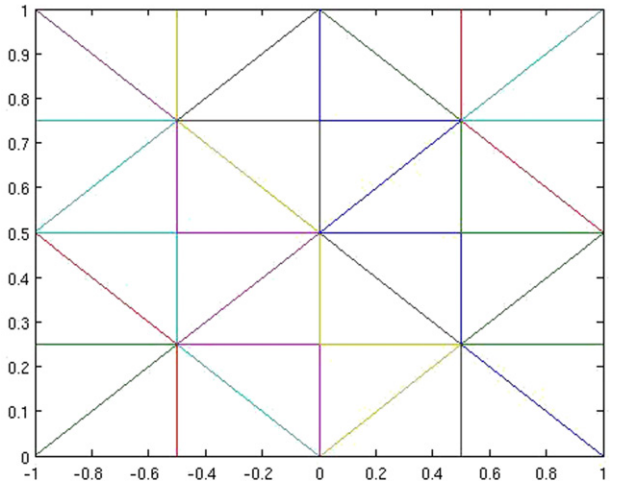


**Fig. 5.1.** Computational mesh corresponding to $h = 1/4$.

**Table 5.1**
Experimental convergence rates for the $(RT_0, \text{disc}P_0)$ approximation pair.

| $1/h$ | $\|\mathbf{u}-\mathbf{u}_h\|_{L^2(\Omega)}$ | Cvg. rate | $\|\text{div}(\mathbf{u}_h)\|_{L^2(\Omega)}$ | $\|p-p_h\|_{L^2(\Omega)}$ | Cvg. rate |
|---|---|---|---|---|---|
| 4 | 3.706E−1 | 0.99 | 8.96E−16 | 4.168E−1 | 1.00 |
| 6 | 2.476E−1 | 1.00 | 3.92E−15 | 2.778E−1 | 1.00 |
| 8 | 1.856E−1 | 1.00 | 1.82E−15 | 2.083E−1 | 1.00 |
| 12 | 1.236E−1 | | 6.45E−15 | 1.389E−1 | |
| Pred. rate | | 1.00 | | | 1.00 |

$$\mathbf{u}_h \cdot \mathbf{n}_e|_{\mathbf{g}} = \frac{length(\hat{\mathbf{e}}_{iT})}{length(\mathbf{e}_i)} c_{\mathbf{g}}, \tag{5.4}$$

where $c_{\mathbf{g}}$ denotes the coefficient $c_k$ in (5.3) associated with the nodal point $\mathbf{g}$.

Consider now $e_{ij}$. From (5.4)

$$\lim_{(x,y)\in T_i \to \mathbf{g}} \mathbf{u}_h \cdot \mathbf{n}_e = \frac{length(\hat{\mathbf{e}}_{iT_i})}{length(\mathbf{e}_i)} c_{\mathbf{g}},$$

$$\text{and} \quad \lim_{(x,y)\in T_j \to \mathbf{g}} \mathbf{u}_h \cdot \mathbf{n}_e = \frac{length(\hat{\mathbf{e}}_{iT_j})}{length(\mathbf{e}_i)} c_{\mathbf{g}}.$$

Continuity of $\mathbf{u}_h \cdot \mathbf{n}$ across $e_{ij}$ requires that $length(\hat{\mathbf{e}}_{iT_i}) = length(\hat{\mathbf{e}}_{iT_j})$. Thus whenever an edge in the triangulation is mapped to the reference triangle its image must be the same size. This restriction does not impose a constraint on the triangulation, but rather on the numerical implementation. (See the *Important Remark* at the end of Section 2.)

### 5.2. Example

Consider the numerical approximation of

$$\mathbf{u} + \eta \nabla p = \mathbf{f}, \quad \text{in } \Omega, \tag{5.5}$$

$$\nabla \cdot \mathbf{u} = 0, \quad \text{in } \Omega, \tag{5.6}$$

$$\mathbf{u} \cdot \mathbf{n} = g, \quad \text{on } \partial\Omega. \tag{5.7}$$

**Remark.** From (5.6), $g$ must satisfy the compatibility condition $\int_{\partial\Omega} g\, ds = 0$.

We consider (5.5)–(5.7) for $\Omega = (-1, 1) \times (0, 1)$, $\eta = 1$, and known solution $\mathbf{u} = \begin{bmatrix} xy - y^2 \\ x + x^2 - 0.5y^2 \end{bmatrix}$, $p = 2x + 3y - 3/2$. For approximating elements we use $(\mathbf{u}_h, p_h) \in (RT_0, \text{disc}P_0)$, $(\mathbf{u}_h, p_h) \in (RT_1, \text{disc}P_1)$, $(\mathbf{u}_h, p_h) \in (RT_2, \text{disc}P_2)$, $(\mathbf{u}_h, p_h) \in (BDM_1, \text{disc}P_0)$ and, $(\mathbf{u}_h, p_h) \in (BDM_2, \text{disc}P_1)$, where

$$\text{disc}P_k = \text{disc}P_k(\Omega) := \{q \mid q \in P_k(T) \forall T \in \mathcal{T}_h\}.$$

The numerical results on a series of meshes are presented in Tables 5.1–5.5. The mesh corresponding to $h = 1/4$ is given in Fig. 5.1.

**Table 5.2**
Experimental convergence rates for the ($RT_1$, disc$P_1$) approximation pair.

| $1/h$ | $\|\mathbf{u}-\mathbf{u}_h\|_{L^2(\Omega)}$ | Cvg. rate | $\|\mathrm{div}(\mathbf{u}_h)\|_{L^2(\Omega)}$ | $\|p-p_h\|_{L^2(\Omega)}$ | Cvg. rate |
|---|---|---|---|---|---|
| 4 | 2.833E−2 | 2.00 | 5.16E−14 | 5.398E−4 | 2.97 |
| 6 | 1.258E−2 | 2.00 | 2.74E−13 | 1.617E−4 | 2.98 |
| 8 | 7.073E−3 | 2.00 | 7.04E−13 | 6.858E−5 | 2.99 |
| 12 | 3.142E−3 | | 5.03E−12 | 2.042E−5 | |
| Pred. rate | | 2.00 | | | 2.00 |

**Table 5.3**
Experimental convergence rates for the ($RT_2$, disc$P_2$) approximation pair.

| $1/h$ | $\|\mathbf{u}-\mathbf{u}_h\|_{L^2(\Omega)}$ | Cvg. rate | $\|\mathrm{div}(\mathbf{u}_h)\|_{L^2(\Omega)}$ | $\|p-p_h\|_{L^2(\Omega)}$ | Cvg. rate |
|---|---|---|---|---|---|
| 4 | 1.047E−13 | | 8.60E−14 | 6.612E−14 | |
| 6 | 1.677E−13 | | 2.16E−13 | 6.965E−14 | |
| 8 | 1.943E−13 | | 6.95E−13 | 7.056E−14 | |
| 12 | 1.008E−12 | | 2.14E−12 | 8.421E−14 | |
| Pred. rate | | – | | | – |

**Table 5.4**
Experimental convergence rates for the ($BDM_1$, disc$P_0$) approximation pair.

| $1/h$ | $\|\mathbf{u}-\mathbf{u}_h\|_{L^2(\Omega)}$ | Cvg. rate | $\|\mathrm{div}(\mathbf{u}_h)\|_{L^2(\Omega)}$ | $\|p-p_h\|_{L^2(\Omega)}$ | Cvg. rate |
|---|---|---|---|---|---|
| 4 | 2.833E−2 | 2.00 | 7.89E−16 | 4.167E−1 | 1.00 |
| 6 | 1.258E−2 | 2.00 | 2.13E−15 | 2.778E−1 | 1.00 |
| 8 | 7.073E−3 | 2.00 | 1.75E−15 | 2.083E−1 | 1.00 |
| 12 | 3.142E−3 | | 5.29E−15 | 1.389E−1 | |
| Pred. rate | | 2 | | | 1 |

**Table 5.5**
Experimental convergence rates for the ($BDM_2$, disc$P_1$) approximation pair.

| $1/h$ | $\|\mathbf{u}-\mathbf{u}_h\|_{L^2(\Omega)}$ | Cvg. rate | $\|\mathrm{div}(\mathbf{u}_h)\|_{L^2(\Omega)}$ | $\|p-p_h\|_{L^2(\Omega)}$ | Cvg. rate |
|---|---|---|---|---|---|
| 4 | 1.038E−13 | | 3.08E−15 | 4.235E−14 | |
| 6 | 1.100E−13 | | 5.91E−15 | 4.349E−14 | |
| 8 | 1.132E−13 | | 8.68E−15 | 4.384E−14 | |
| 12 | 1.165E−13 | | 1.64E−14 | 4.423E−14 | |
| Pred. rate | | – | | | – |

## 6. Concluding remarks

In this article we have introduced a computational basis for the $RT_k$ and $BDM_k$ approximating elements on a triangulation of the domain $\Omega \subset \mathbb{R}^2$. Our computational basis imposes a minor restriction on the mapping of the triangles in the triangulation to the reference triangle $\widehat{T}$ (see *Important Remark* at the end of Section 2). This restriction can be removed if instead of $\widehat{T}$ given by (0, 0), (1, 0), (0, 1) one uses $\widehat{T}_{eq}$ given by $(-1, 0)$, (0, 1), $(0, \sqrt{3})$. The corresponding bases on $\widehat{T}_{eq}$ can be obtained by applying the Piola transformation to the bases defined above. Alternatively, as pointed out by Walkington [9], this restriction can be removed and $\widehat{T}$ still used as the reference triangle if the Piola transformation (2.7) is modified for Normal Basis Functions to compensate for the factor $length(\hat{\mathbf{e}}_{iT})/length(\mathbf{e}_i)$.

## References

[1] F. Brezzi, M. Fortin, Mixed and Hybrid Finite Element Methods, Springer-Verlag, New York, 1991.
[2] C. Bahriawati, C. Carstensen, Three MATLAB implementations of the lowest-order Raviart–Thomas MFEM with a posteriori error control, Comput. Methods Appl. Math. 5 (4) (2005) 333–361 (electronic).
[3] F. Hecht, O. Pironneau, Freefem++, webpage: http://www.freefem.org.
[4] D.N. Arnold, R.S. Falk, R. Winther, Geometric decompositions and local bases for spaces of finite element differential forms, Comput. Methods Appl. Mech. Engrg. 198 (21–26) (2009) 1660–1672.
[5] M. Ainsworth, J. Coyle, Hierarchic finite element bases on unstructured tetrahedral meshes, Internat. J. Numer. Methods Engrg. 58 (14) (2003) 2103–2130.
[6] J. Schöberl, S. Zaglmayr, High order Nédélec elements with local complete sequence properties, COMPEL 24 (2) (2005) 374–384.
[7] R.H.W. Hoppe, Finite Element Methods—Course Notes, Technical Report, Department of Mathematics, University of Houston, 2005. http://www.math.uh.edu/~rohop/spring_05/downloads/Chapter7.pdf (Chapter 7).
[8] F.-J. Sayas, A gentle introduction to the Finite Element Method—Course Notes, Technical Report, Department of Mathematical Sciences, University of Delaware, 2008. http://www.math.udel.edu/~fjsayas/anIntro2FEM.pdf.
[9] N. Walkington, Personal communication, 2011.